

## High-Harmonic Generation with Combined Infrared and Extreme Ultraviolet Fields

M. Tudorovskaya<sup>a\*</sup> and M. Lein<sup>a</sup>

<sup>a</sup>*Institut für Theoretische Physik and Centre for Quantum Engineering and Space-Time Research (QUEST), Leibniz Universität Hannover, Appelstraße 2, D-30167 Hannover, Germany*

(July 27, 2013)

High-order harmonic generation (HHG) is a nonlinear optical process usually interpreted as a sequence of ionization of an atom or molecule by a strong laser field and the following recombination under emission of an extreme ultraviolet photon. We investigate HHG for combined infrared and extreme ultraviolet fields acting on a system possessing two essential states, with the excited state being either a bound state or a resonance. We report shifts of the HHG peak positions compared to the HHG spectrum from an infrared field only and a peak splitting depending on the presence of Rabi oscillations.

**Keywords:** high harmonic generation; Rabi oscillations; two-level system

### 1. Introduction

High-order harmonic generation (HHG) is the nonlinear process taking place when an atomic or molecular target is subjected to a strong laser field. Powerful infrared (IR) lasers such as the Ti:sapphire laser are available and commonly used in HHG experiments. In the tunneling regime [1], i.e. at low frequencies of the driving field  $\omega_0$  and high field amplitude  $E_0$ , HHG can be described in terms of the three-step model [2]. According to the model, the first step is the tunneling ionization of the target, the second step is the acceleration of the electron driven by the laser field, and the third step is the recombination with the parent ion with emission of extreme ultraviolet (XUV) light. The maximum energy of the returning electrons is  $3.17U_p$  where  $U_p = E_0^2/(4\omega_0^2)$  is the ponderomotive energy. Thus, denoting the ionization potential as  $I_p$ , the HHG spectrum has a cutoff at

$$\omega_{\text{cutoff}} = 3.17U_p + I_p. \quad (1)$$

For inversion symmetric systems such as atoms, the plateau of the HHG spectrum consists of peaks at odd orders of the laser frequency due to the periodicity of the laser field,

$$\omega_n = (2n + 1)\omega_0, n \in \mathbb{N}. \quad (2)$$

A usual assumption is that the ground state is the only bound state involved in this process [3]. In general, real quantum systems have more than one bound electronic state, but a moderate nonresonant IR field is not normally assumed to lift significant population into bound excited

---

\*Corresponding author. Email: maria.tudorovskaya@itp.uni-hannover.de

states that would contribute to HHG. However, if a near-resonant ultraviolet or extreme ultraviolet (XUV) field with frequency  $\omega_{\text{XUV}}$  is additionally applied, excited states are expected to be populated as well, which may cause drastic changes in the HHG spectrum.

Let us consider a system with just two bound electronic states. The ground-state energy is  $\mathcal{E}_g$  and the excited-state energy is  $\mathcal{E}_e$ , so the levels are separated by the excitation energy  $\Delta = \mathcal{E}_e - \mathcal{E}_g$ . If the detuning  $\delta$  between the XUV frequency and  $\Delta$  is small,

$$|\delta| = |\omega_{\text{XUV}} - \Delta| \ll \Delta, \quad (3)$$

the excited state can be populated efficiently by the XUV field. If the duration of the XUV field is sufficiently long, the population oscillates with the Rabi frequency  $\Omega_R$ ,

$$\Omega_R = \sqrt{|d_E|^2 + \delta^2}, \quad (4)$$

where  $d_E = \langle \Psi_g | x | \Psi_e \rangle E_{\text{XUV}}$  is the transition matrix element for the interaction with an XUV field of amplitude  $E_{\text{XUV}}$ . If only the ground state is populated at  $t=0$ , the excited-state population oscillates as

$$A_R(t) = \frac{|d_E|^2}{\Omega_R^2} \sin^2 \left( \frac{\Omega_R t}{2} \right). \quad (5)$$

The ground-state population is  $1 - A_R(t)$  if the excited state does not decay via other channels.

HHG from infrared irradiation supported by additional fields has been studied experimentally and theoretically. It has been suggested to use attosecond pulses obtained by HHG from a secondary source as an auxiliary XUV field to enhance HHG [4, 5]. Experimentally, a mixture of Xe and He was used to observe dramatic enhancement of harmonic generation in He boosted by the harmonic field produced by Xe [6, 7]. Another experiment showed enhancement by one order of magnitude in He using attosecond pulse trains from a Xe-filled capillary [8]. A dual-gas-cell setup has been investigated in [9]. Propagation effects have been simulated in detail [10, 11] and more theoretical work has been reported in [12, 14]. Buth *et al.* [15, 16] coupled the two-electron problem with the problem of XUV-assisted HHG in gases such as Ne and Kr, considering conditions as at the free electron laser FLASH in Hamburg. The authors have developed a theoretical formalism and discovered a second plateau in the HHG spectrum as a result of electron recombination with a core hole.

In our present work we numerically investigate two-colour driven HHG with different types of XUV pulses. We choose the parameters such that Rabi oscillations can be induced by the XUV field. We consider systems with either a stable or a metastable excited state and discuss the influence of the excited-state lifetime on the HHG spectrum.

## 2. Methods

Atomic units are used throughout the paper. We numerically solve the one-dimensional time-dependent Schrödinger equation (TDSE) in the single-active-electron approximation for a model potential  $V_0$ . The unperturbed Hamiltonian  $H_0$  has eigenstates  $\Psi_g$  and  $\Psi_e$  with

$$H_0 \Psi_{e,g} = \mathcal{E}_{e,g} \Psi_{e,g}. \quad (6)$$

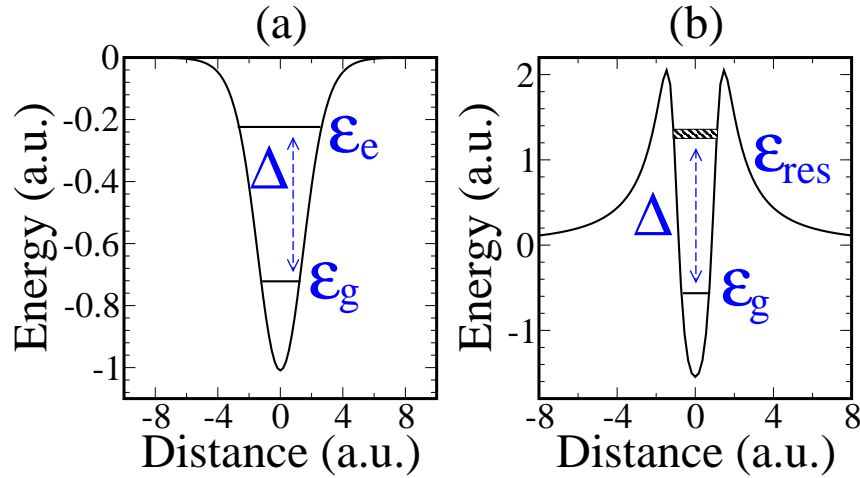


Figure 1. (a) Model potential with two bound states, ground-state energy  $\mathcal{E}_g = -0.717$  a.u. and excited-state energy  $\mathcal{E}_e = -0.240$ . (b) Model potential with a shape resonance, ground-state energy  $\mathcal{E}_g = -0.571$  a.u., resonance energy  $\mathcal{E}_{\text{res}} = 1.332$ , width  $\Gamma = 0.1$  a.u. and decay time  $T_{\text{decay}} = 10$  a.u.

When the system is exposed to the electric field  $E(t)$ , the TDSE in length gauge reads

$$i \frac{\partial \Psi(x, t)}{\partial t} = -\frac{1}{2} \frac{\partial^2 \Psi(x, t)}{\partial x^2} + (V_0(x) + E(t)x) \Psi(x, t). \quad (7)$$

The equation is numerically solved using the split-operator technique [17]. The resulting HHG spectrum  $S(\omega)$  is obtained from the Fourier transform of the dipole acceleration,

$$S(\omega) \propto |\tilde{a}(\omega)|^2 = \left| \int dt \left\langle \Psi(t) \left| \frac{dV_0(x)}{dx} + E(t) \right| \Psi(t) \right\rangle e^{i\omega t} \right|^2. \quad (8)$$

We use two types of model potentials as shown in figure 1. The first type,  $V_0^{21}$ , is a simple potential well supporting two bound electronic states. The second type,  $V_0^{\text{res}}$ , has potential barriers at the edges of the well such that the excited state is an autoionizing shape resonance with a width  $\Gamma$  and lifetime  $T_{\text{decay}} = 1/\Gamma$ . Such a potential can be used to model HHG in real systems with autoionizing resonances, for instance, in a Mn plasma [18]. The potentials read

$$V(x) = -\alpha_1 + \frac{\alpha_1}{1 + e^{\frac{x+\alpha_2}{\alpha_3}}} + \frac{\alpha_1}{1 + e^{\frac{-x+\alpha_2}{\alpha_3}}} + \frac{\alpha_4}{(\alpha_5 + x^2)(1 + e^{\frac{x+\alpha_2}{\alpha_3}})} + \frac{\alpha_4}{(\alpha_5 + x^2)(1 + e^{\frac{-x+\alpha_2}{\alpha_3}})}. \quad (9)$$

where  $\alpha_i$  with  $i \in \{1, \dots, 5\}$  are parameters chosen such that only two states are present.

All employed external fields are of the form  $E(t) = E_0 \sin(\omega_0 t) f(t)$ , where  $f(t)$  is the envelope. The envelope is chosen such that the pulses consist of an integer number of optical cycles. The wavelength of the infrared field is 765 nm, corresponding to  $\omega_0 = 0.06$  a.u. The duration of the IR pulse is 1465.3 a.u., which corresponds to 14 optical cycles. To investigate the influence of the excited-state lifetime, we use two types of XUV pulses: an ultrashort XUV pulse lasting less than half an IR period and a long XUV pulse with a duration comparable with the IR pulse length. In the following, we refer to the short and long pulses as ‘XUV<sub>s</sub>’ and ‘XUV<sub>l</sub>’, respectively. In case of the two-bound-level system with potential  $V_0^{21}$ , we use a near-resonant XUV field with frequency 0.51 a.u. In case of the potential  $V_0^{\text{res}}$  with the shape resonance, the

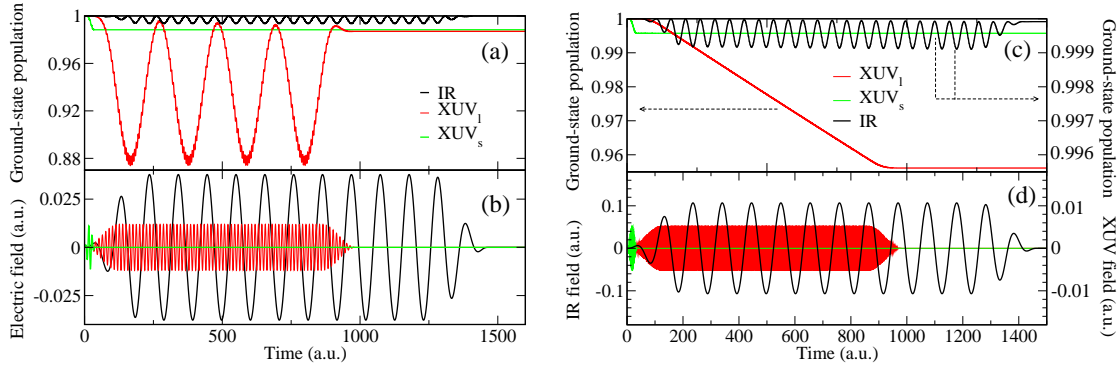


Figure 2. Left: Results for the two-bound-level system. Right: Results for the shape resonance. (a), (c) Population of the ground state when the system is driven by the XUV field only or by the IR field only. (b) The IR field and the XUV field used in the case of the two-bound-level system; the intensities of the IR and XUV fields are  $5 \times 10^{13}$  W/cm<sup>2</sup> and  $5 \times 10^{12}$  W/cm<sup>2</sup>, respectively; the XUV<sub>I</sub> and XUV<sub>S</sub> pulses consist of 10+60+10 and 3 optical cycles, respectively; the XUV frequency is 0.51 a.u. (d) The IR field and the XUV field for the system with a shape resonance; the intensities of the IR and XUV fields are  $4 \times 10^{14}$  W/cm<sup>2</sup> and  $10^{12}$  W/cm<sup>2</sup>, respectively; the XUV<sub>I</sub> and XUV<sub>S</sub> pulses consist of 37+221+37 and 11 optical cycles, respectively; the XUV frequency is 1.88 a.u.

XUV field has the frequency 1.88 a.u. We choose a trapezoidal envelope and duration about 985 a.u. for XUV<sub>I</sub>. The ramps and the plateau lengths are 10+60+10 optical XUV cycles for the 0.51 a.u. field and 37+221+37 in the case of the 1.88 a.u. field. The duration of XUV<sub>S</sub> is about 37 a.u., corresponding to three optical cycles of the 0.51 a.u. field and 11 optical cycles of the 1.88 a.u. field. The XUV<sub>S</sub> envelope has a sin<sup>2</sup> shape. The short pulse can be viewed as a single attosecond pulses produced by HHG from a different gas target. The long pulse models an XUV field produced by, for example, FLASH with a duration of 10-50 fs (FWHM). The numerical propagation is continued for two more IR cycles after the IR pulse is over to ensure that all relevant electron wavepackets have returned to the core.

### 3. Results and discussion

#### 3.1. Response to the XUV field only and IR field only

In this section, we discuss the response of the quantum system to the XUV field only and to the IR field only. For  $V_0^{21}$  with  $\Delta = 0.48$  a.u., we set the IR intensity to  $5 \times 10^{13}$  W/cm<sup>2</sup> and the XUV intensity to  $5 \times 10^{12}$  W/cm<sup>2</sup>. In the case of the potential with a shape resonance,  $V_0^{\text{res}}$ , the excitation energy is  $\Delta = 1.9$  a.u., the IR intensity is  $4 \times 10^{14}$  W/cm<sup>2</sup>, and the XUV intensity is  $10^{12}$  W/cm<sup>2</sup>. At time  $t=0$ , the system is in the ground state and the field is switched on. The left-hand side of figure 2 applies to the system with two bound states and the right-hand side applies to the system with a shape resonance. The bottom panels show the XUV and IR fields used in the calculation. The top panels show the corresponding time-dependent population of the ground state when exposed to the XUV field only or IR field only (not combined). In the IR field, the population oscillates with a period equal to half of the IR period for both  $V_0^{21}$  and  $V_0^{\text{res}}$ . This can be understood as a consequence of an instantaneous IR-dressed ground state that differs from the field-free ground state. The overlap with the field-free state is thus less than one and oscillates with the IR field.

Figure 2(a) shows that the long XUV pulse causes Rabi oscillations in the ground-state population of the two-level system. The corresponding oscillations of the excited-state population (not shown) are in antiphase to the ground-state oscillations. In contrast, the short XUV pulse is shorter than the Rabi period, and its main effect is a quick transfer of a small population to the excited state without Rabi oscillations.

For  $V_0^{\text{res}}$  (figure 2, right hand side), no Rabi oscillations can be observed even when the XUV pulse is sufficiently long. This is due to the fast decay of the resonance state.

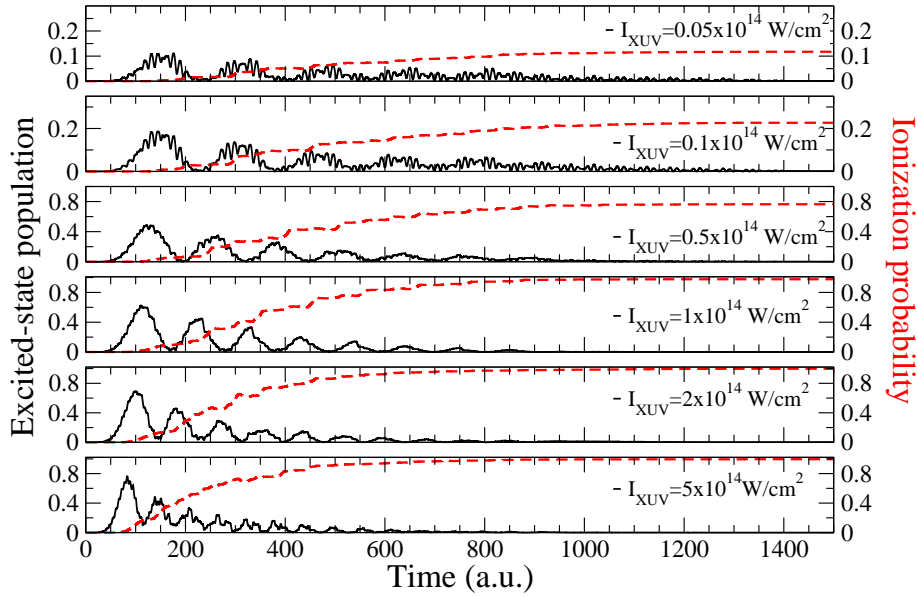


Figure 3. Population of the excited state (black solid curve) and the ionization probability (red dashed curve) for the system with two bound states driven by combination of the IR field and the long XUV pulse for various XUV intensities.

### 3.2. System with two bound states

First, we show the Rabi oscillations caused by the combination of the long XUV pulse ( $XUV_l$ ) and the IR field. Figure 3 shows that at any of the considered XUV intensities, from  $5 \times 10^{12}$  to  $5 \times 10^{14}$  W/cm<sup>2</sup>, excited-state population oscillations are observed. The amplitude and the frequency of the oscillations (black curve) increase with increasing intensity as well as the ionization probability (red curve). The amplitude of the oscillations decays with time, even when the XUV intensity is low, in contrast to the case where the system is driven by the XUV field only, see figure 2(a). For high XUV intensity, the decay of the oscillations is due to the strong ionization. For low XUV intensity, the decay is apparently due to the presence of the IR field. The upper state is ionized easily by the IR field, so the presence of the IR field is effectively causing a finite lifetime of the upper state.

Next, we consider the effect of the excited-state population on the HHG spectrum. Figure 4 shows the HHG spectra produced by the IR field alone (black curve),  $XUV_l$  alone (dashed purple curve) and in case of simultaneous irradiation of the IR and XUV fields, both for the  $XUV_s$  pulse (green curve) and the  $XUV_l$  pulse (red curve). The IR field with intensity  $I = 5 \times 10^{13}$  W/cm<sup>2</sup> corresponds to the ponderomotive potential  $U_p = E_0^2/(4\omega_0^2) = 0.10$  a.u., and the cutoff in the HHG spectrum by the IR field only is expected at  $3.17U_p + I_p = 1.03$  a.u. We find that compared to the XUV-only case, adding the IR field helps to efficiently produce high-order harmonics in the cutoff region. The emission enhancement is more than 2 orders of magnitude in the peaks for the  $XUV_l$  case. Compared to the IR-only case (black curve), HHG is increased by about 6-8 orders of magnitude when additionally driven by the XUV field, both for  $XUV_l$  and  $XUV_s$ . The increase of the emission occurs due to population of the excited state by the XUV pulse and thus due to the increased probability of ionization as the first step of the three-step model.

The inset of figure 4 is a magnified view of the spectra, showing the exact positions of the peaks. While still being separated by  $2\omega_0$ , the peaks are found to be shifted compared to the usual odd orders  $(2n+1)\omega_0$  of the IR laser frequency. For the short XUV pulse (green curve in figure 4), relatively broad peaks are found at energies

$$\omega_n^{\text{short}} = \Delta + 2n\omega_0. \quad (10)$$

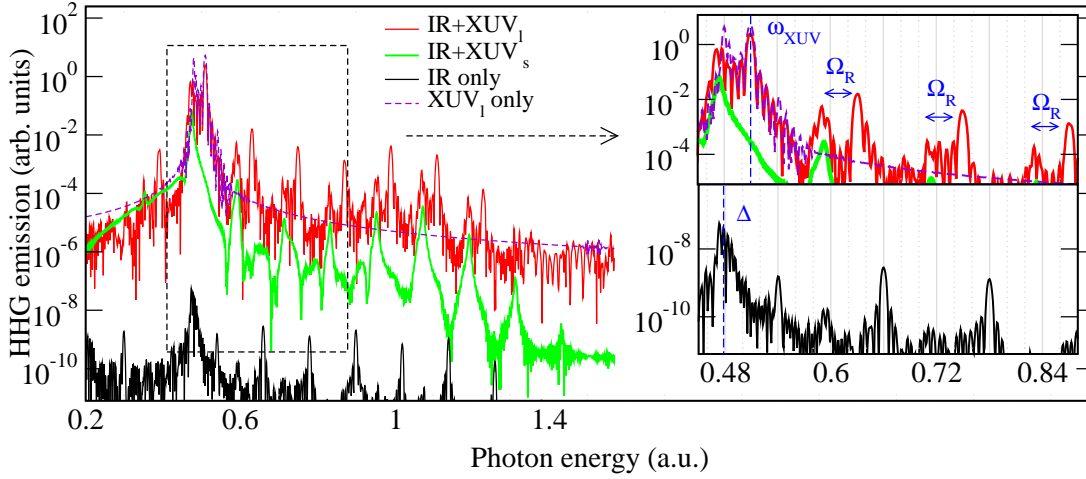


Figure 4. HHG spectra from the system with two bound states, produced by the IR field alone (black curve), by the XUV<sub>l</sub> pulse alone (dashed purple curve), and by the combinations of the IR field with the short XUV (green curve) and long XUV (red curve) pulses. The following field parameters are used. IR:  $\omega_{\text{IR}} = 0.06$  a.u.,  $I_{\text{IR}} = 5 \times 10^{13}$  W/cm<sup>2</sup>. XUV<sub>l</sub>:  $\omega_{\text{XUV}} = 0.51$  a.u., 80 optical cycles,  $I_{\text{XUV}} = 5 \times 10^{12}$  W/cm<sup>2</sup>. XUV<sub>s</sub>:  $\omega_{\text{XUV}} = 0.51$  a.u., 3 optical cycles,  $I_{\text{XUV}} = 5 \times 10^{12}$  W/cm<sup>2</sup>. The insets show enlarged regions of the spectra.

The XUV<sub>s</sub> pulse initially creates a superposition of ground and excited states, so that IR-driven HHG can start from the excited state and finish in the ground state, leading to peaks shifted by  $\Delta$ . When the long XUV pulse is used (red curve in figure 4), the dominating peaks are situated at (cf. [12, 13])

$$\omega_n^{\text{long}} = \omega_{\text{XUV}} + 2n\omega_0 \quad (11)$$

as a result of converting the energy of one XUV photon and  $2n$  IR photons into the energy of the emitted photon. The spectrum generated by XUV<sub>l</sub> only (figure 4, dashed curve) shows that the long XUV pulse causes a Rabi splitting of the emission peak, analogous to the Autler-Townes effect in absorption lines [19] and photoelectron spectra [20]. If the IR field is added, not only the peak at  $\omega_{\text{XUV}}$ , but also all the higher energy peaks are split: in addition to the dominating emission at  $\omega_n^{\text{long}}$ , secondary peaks at  $\omega_n^{\text{long}} - \Omega_R$  are observed. The reason is the periodicity of the XUV-induced Rabi oscillations.

### 3.3. System with a shape resonance

In the case that the excited state is metastable, the question arises whether the enhancement of HHG by simultaneous irradiation of XUV and IR fields persists. We consider HHG from the potential  $V_0^{\text{res}}$  with a short decay time of 10 a.u. of the upper state. In this model, the upper state is a shape resonance.

As in the previous section, we first show the excited-state population and ionization dynamics for various XUV intensities of the long XUV pulse, see figure 5. The frequency of the oscillation envelope equals twice the IR frequency. It does not depend on the intensity of the XUV field. The oscillations are not Rabi oscillations, because the upper state decays quickly into an ion and a free electron. Rather, the oscillations are caused by dressing of the electronic states by the applied instantaneous field. The ionization is almost entirely caused by the XUV-induced excitation followed by decay of the metastable state.

We calculate HHG emission with an XUV intensity of  $10^{12}$  W/cm<sup>2</sup>. Figure 6 shows the result of the numerical simulation. The black curve is the HHG spectrum from the IR field only. The emission is in the form of odd orders of the IR frequency and it is strongest around the resonant energy  $\Delta = 1.9$  a.u. When the XUV field is added, we observe the following effect. If the XUV

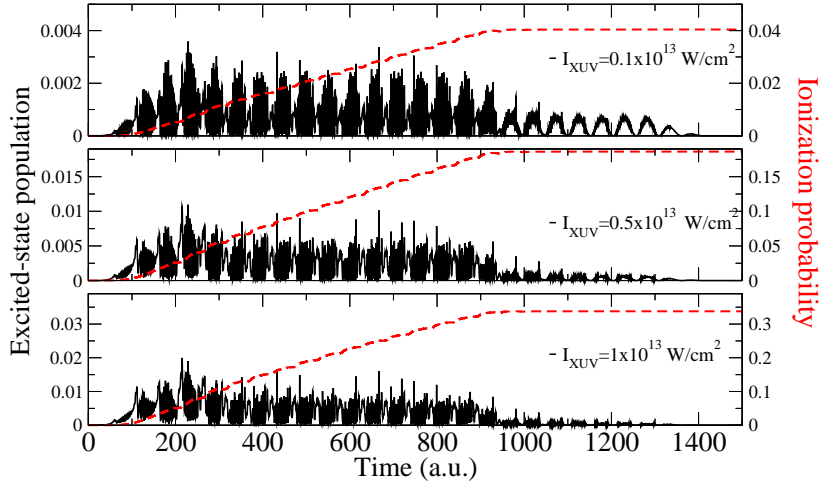


Figure 5. Population of the excited state (black solid curve) and the ionization probability (red dashed curve) for the system with a shape resonance driven by combination of the IR field and the long XUV pulse for various XUV pulse intensities.

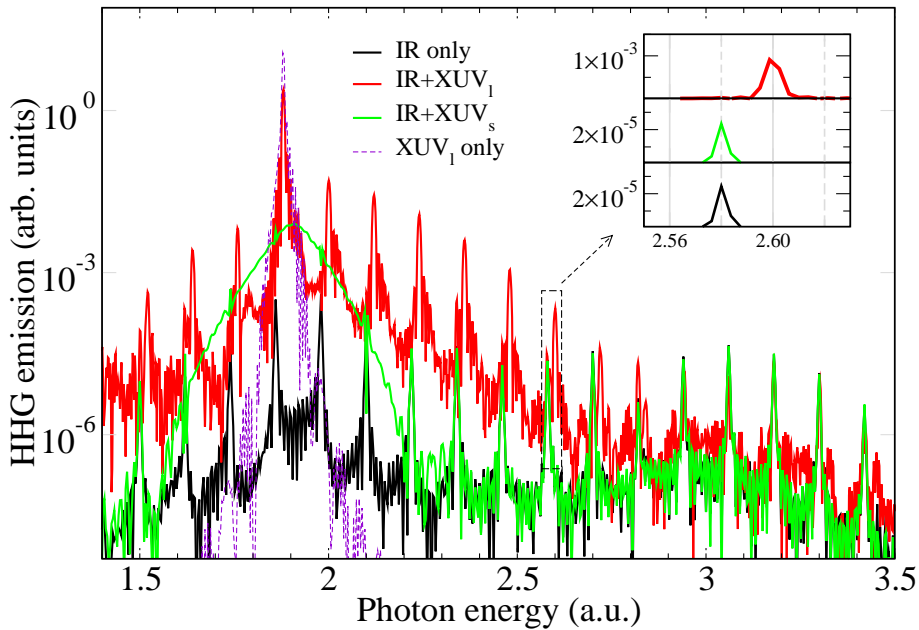


Figure 6. HHG spectra from a system with a shape resonance produced by the IR field alone (black curve), by the  $XUV_l$  pulse alone (dashed purple curve), and by the combined fields IR +  $XUV_l$  and IR +  $XUV_s$ . The insets show magnified parts of the spectra. The following field parameters are used. IR:  $\omega_{IR} = 0.06$  a.u.,  $I_{IR} = 4 \times 10^{14}$  W/cm<sup>2</sup>.  $XUV_l$ :  $\omega_{XUV} = 1.88$  a.u., 295 optical cycles,  $I_{XUV} = 10^{12}$  W/cm<sup>2</sup>.  $XUV_s$ :  $\omega_{XUV} = 1.88$  a.u., 11 optical cycles,  $I_{XUV} = 10^{12}$  W/cm<sup>2</sup>.

pulse is short ( $XUV_s$  case), only the resonant region emission is enhanced compared to the IR-only case. We observe a broad peak at the energy  $\Delta = 1.9$  a.u. Since the metastable state decays with the lifetime 10 a.u. after it has been initially populated by the  $XUV_s$  pulse, the electron emission from the excited state is not periodic, and no harmonic structure is observed. At frequencies above the resonance, the signal coincides with the IR-only HHG spectrum. If the XUV pulse is long ( $XUV_l$ ), it causes continuous repopulation of the metastable state. The intensity of the HHG emission exceeds the IR-only spectrum by about 2-3 orders of magnitude. The peak positions are consistent with equation (11). There is, however, no Rabi splitting of the peaks since the lifetime of the resonance is shorter than the Rabi period.

#### 4. Conclusions

In this paper, we have investigated the generation of high harmonics driven by an IR field assisted by an XUV field. We have shown that in a quantum system with a bound or metastable excited electronic state, adding a moderate near-resonant XUV pulse can lead to enormous enhancement of the HHG emission due to XUV-induced population of the excited state, from which the IR field can drive HHG more easily than from the ground state. The resulting radiation exceeds both the HHG signal from IR-only and from XUV-only fields. The positions of the harmonic peaks are shifted away from odd orders of the IR frequency. The details of the resulting HHG spectrum depend on the lifetime of the excited state. If the XUV pulse is sufficiently long and the excited-state lifetime is longer than the corresponding Rabi period, Rabi splitting of the harmonic peaks is observed in the HHG spectrum.

#### 5. Acknowledgments

We acknowledge the support from the European Marie Curie Initial Training Network Grant No. CA-ITN-214962-FASTQUAST. We thank the Deutsche Forschungsgemeinschaft for funding the Centre for Quantum Engineering and Space-Time Research (QUEST).

#### References

- [1] Keldysh, L.V. Ionization in the field of a strong electromagnetic wave. *Sov. Phys. JETP* **1965**, *20*, 1307–1314.
- [2] Corkum, P.B. Plasma perspective on strong field multiphoton ionization. *Phys. Rev. Lett.* **1993**, *71*, 1994–1997.
- [3] Lewenstein, M.; Balcou, P.; Ivanov, M.Y.; L’Huillier, A.; Corkum, P.B. Theory of high-harmonic generation by low-frequency laser fields. *Phys. Rev. A* **1994**, *49*, 2117–2132.
- [4] Bandrauk, A.D.; Shon, N.H.; Attosecond control of ionization and high-order harmonic generation in molecules. *Phys. Rev. A* **2002**, *66*, 031401(R).
- [5] Ishikawa, K. Photoemission and Ionization of He<sup>+</sup> under Simultaneous Irradiation of Fundamental Laser and High-Order Harmonic Pulses. *Phys. Rev. Lett.* **2003**, *91*, 043002.
- [6] Takahashi, E.J.; Nabekawa, Y.; Mashiko, H.; Hasegawa, H.; Suda, A.; Midorikawa, K. Generation of strong optical field in soft X-ray region by using high-order harmonics. *IEEE J. Sel. Top. Quantum Electron.* **2004**, *10*, 1315–1328.
- [7] Takahashi, E.J.; Kanai, T.; Ishikawa, K.L.; Nabekawa, Y.; Midorikawa, K. Dramatic Enhancement of High-Order Harmonic Generation. *Phys. Rev. Lett.* **2007**, *99*, 053904.
- [8] Biegert, J.; Heinrich, A.; Hauri, C.P.; Kornelis, W.; Schlup, P.; Anscombe, M.P.; Gaarde, M.B.; Schafer, K.J.; Keller, U. Control of high-order harmonic emission using attosecond pulse trains. *J. Mod. Opt.* **2006**, *53*, 87–96.
- [9] Brizuela, F.; Heyl C.M.; Rudawski P.; Kroon, D.; Rading, L.; Dahlström, J.M.; Mauritsson J.; Johnsson, P.; Arnold, C.L.; L’Huillier, A. Efficient high-order harmonic generation boosted by below-threshold harmonics. *Sci. Rep.* **2013**, *3*, 1410.
- [10] Gaarde, M.B.; Schafer, K.J.; Heinrich, A.; Biegert, J.; Keller, U. Large enhancement of macroscopic yield in attosecond pulse train-assisted harmonic generation. *Phys. Rev. A* **2005**, *72*, 013411.
- [11] Schiessl, K.; Persson E.; Scrinzi, A.; Burgdörfer, J. Enhancement of high-order harmonic generation by a two-color field: Influence of propagation effects. *Phys. Rev. A* **2006**, *74*, 053412.
- [12] Fleischer, A.; Moiseyev, N. Amplification of high-order harmonics using weak perturbative high-frequency radiation. *Phys. Rev. A* **2008**, *77*, 010102(R).
- [13] Fleischer, A. Generation of higher-order harmonics upon the addition of high-frequency XUV radiation to IR radiation: Generalization of the three-step model. *Phys. Rev. A* **2008**, *78*, 053413.
- [14] Popruzhenko, S.V.; Zaretsky, D.F.; Becker, W. High-order harmonic generation by an intense infrared laser pulse in the presence of a weak UV pulse. *Phys. Rev. A* **2010**, *81*, 063417.
- [15] Buth, C.; Kohler, M.C.; Ullrich, J.; Keitel, C.H. High-order harmonic generation enhanced by XUV light. *Opt. Letters* **2011**, *36*, 3530–3532.
- [16] Buth, C. High-order harmonic generation with resonant core excitation by ultraintense x rays. *arXiv:1303.1332* **2013**.
- [17] Feit, M.D.; Fleck, J.A., Jr.; Steiger, A. Solution of the Schrödinger equation by a spectral method. *Journal of Computational Physics* **1982**, *47*, 412 – 433.
- [18] Ganeev, R.A.; Witting, T.; Hutchison, C.; Frank, F.; Tudorovskaya, M.; Lein, M.; Okell, W.A.; Zair, A.; Marangos, J.P.; Tisch, J.W.G. Isolated sub-fs XUV pulse generation in Mn plasma ablation. *Opt. Express* **2012**, *20*, 25239–25248.
- [19] Autler, S.H.; Townes, C.H. Stark Effect in Rapidly Varying Fields. *Phys. Rev.* **1955**, *100*, 703–722.
- [20] Wollenhaupt, M.; Assion, A.; Bazhan, O.; Horn, C.; Liese, D.; Sarpe-Tudoran, C.; Winter, M.; Baumert, T. Control of interferences in an Autler-Townes doublet: Symmetry of control parameters. *Phys. Rev. A* **2003**, *68*, 015401(R).